iScience

CellPress
OPEN ACCESS

Article

Once-monthly hemin suppresses inflammatory and autoreactive CD4$^+$ T cell responses to robustly ameliorate experimental rheumatoid arthritis

Bingzhi Sun, Gaojie Li, Ling Guo, ..., Xiaodong Wu, Runyue Huang, Min Feng

guoling7@mail.sysu.edu.cn (L.G.)
ryhuang@gzucm.edu.cn (R.H.)
fengmin@mail.sysu.edu.cn (M.F.)

Highlights

Repurposing hemin prevents the onset and ameliorates the clinical course of RA

Once-monthly hemin achieve sustained remission of RA for at least six weeks

Hemin rescue dysregulated gene expression and attenuate autoreactive immune responses

Sun et al., iScience *24*, 103101
October 22, 2021
https://doi.org/10.1016/j.isci.2021.103101

iScience

CellPress
OPEN ACCESS

Article

Once-monthly hemin suppresses inflammatory and autoreactive CD4$^+$ T cell responses to robustly ameliorate experimental rheumatoid arthritis

Bingzhi Sun,[1,2] Gaojie Li,[1,2] Ling Guo,[1,2,*] Na Yin,[1,2] Huan Huang,[1,2] Xiaodong Wu,[3,4] Runyue Huang,[3,4,*] and Min Feng[1,2,5,*]

SUMMARY

Rheumatoid arthritis (RA) is an inflammatory autoimmune disease that would permanently damage the affected joints. Unfortunately, a large proportion of RA patients fail to respond adequately to current treatments. Here, repurposing hemin and its ultra-long-acting formulation were explored for the effective treatment of RA in animal models. We provided evidence that hemin prevented the onset and ameliorated the clinical course of RA. Notably, hemin treatment rescued the dysregulated gene expression in animal models of RA, resulting in attenuation of Th1/Th17 cell-mediated responses and proinflammatory cytokines. Moreover, we further formulated hemin into the *in-situ* forming implant, and a single injection of the ultra-long-acting hemin exerted potent disease-modifying effects for at least six weeks with a remarkable dose reduction. Taken together, given the potent anti-inflammatory and immunosuppressive effects, the once-monthly hemin injection holds promise for rapid clinical translation, and represents a potential strategy to treat RA and possibly other autoimmune diseases.

INTRODUCTION

Rheumatoid arthritis (RA) is a severe chronic autoimmune disease that can cause joint pain, stiffness, and progressive structural damage (Smolen et al., 2016). The current recommendations address treatment of RA consisting mainly of conventional synthetic disease-modifying antirheumatic drugs (DMARDs), biologic DMARDs, targeted synthetic DMARDs, and glucocorticoids (Fraenkel et al., 2021). Among DMARDs, methotrexate is the most commonly prescribed (Ferrara et al., 2018; Brown et al., 2016). Nevertheless, more than 40% of the patients receiving methotrexate treatment do not respond adequately after two years (Nair et al., 2020). When such immunomodulators fail to attain sustained remission or low disease activity, uncontrolled inflammation fuels RA progression and drives joint damage, leading to functional disability and reduced quality of life (Smolen et al., 2016; Ho et al., 2019). The work disability rates in RA patients are up to 42% after six to ten years' disease duration due to the lack of universally effective treatments (Eberhardt et al., 2007). Thus, there remains a significant unmet need in the treatment of RA. The challenge in RA treatment is to develop a new therapy that takes account of both early dominant autoimmunity and later structural damage-related inflammation for improved clinical outcomes (Burmester and Pope, 2017).

As a chronic inflammatory and autoimmune disease, RA is relevant to oxidative stress. There is evidence that inducing heme oxygenase-1 (HO-1), a stress-responsive protein, is considered as an adaptive cytoprotective response against oxidative stress (Wruck et al., 2011). It has been reported that HO-1 is overexpressed in synovium from RA patients, compared with that from healthy donors or osteoarthritis patients (Kobayashi et al., 2006; Kitamura et al., 2011; Yang et al., 2019). In the collagen-induced arthritis (CIA) model, HO-1 induction alleviates joint inflammation and reduces arthritis severity (Yang et al., 2018; Moon et al., 2017; Ferrandiz et al., 2008). Nevertheless, there seems to be contradictory evidence demonstrating that using the HO-1 inducer, cobalt protoporphyrin IX (CoPP), failed to delay the progression of chronic inflammation in animal models of RA (Devesa et al., 2005). Intrigued by the undetermined role of HO-1 inducers in the remission of RA, we explored whether inducing HO-1 by its potent inducer as well as its natural substrate, hemin, could inhibit inflammation and suppress autoimmune reactivity in the treatment of RA.

[1]School of Pharmaceutical Sciences, Sun Yat-sen University, University Town, Guangzhou 510006, P. R. China

[2]Guangdong Provincial Key Laboratory of Chiral Molecule and Drug Discovery, Sun Yat-sen University, Guangzhou 510006, P.R. China

[3]State Key Laboratory of Dampness Syndrome of Chinese Medicine, The Second Affiliated Hospital of Guangzhou University of Chinese Medicine (Guangdong Provincial Hospital of Chinese Medicine), Guangzhou 510120, P. R. China

[4]Guangdong-Hong Kong-Macau Joint Lab on Chinese Medicine and Immune Disease Research, Guangzhou University of Chinese Medicine, Guangzhou 510120, P. R. China

[5]Lead contact

*Correspondence: guoling7@mail.sysu.edu.cn (L.G.), ryhuang@gzucm.edu.cn (R.H.), fengmin@mail.sysu.edu.cn (M.F.)

https://doi.org/10.1016/j.isci.2021.103101

Hemin is an FDA-approved drug for treating acute intermittent porphyria attacks (Siegert and Holt, 2008). Repurposing existing drugs is an attractive strategy to offer more-effective options to patients, with the substantial advantages of safer, faster, and cheaper preclinical and clinical validation protocols (Bertolini et al., 2015). In the present study, we repurposed hemin for the treatment of RA. We discovered that hemin exerted robust symptomatic and disease-modifying effects in both adjuvant-induced arthritis (AIA) and CIA models. Importantly, hemin rescued the dysregulated gene expression in RA and exerted immunosuppressive effects on autoreactive $CD4^+$ T helper (Th) cells. The pathogenic $CD4^+IFN\text{-}\gamma^+$ Th1 cell proportion and Th17 cell-related cytokine production in CIA rats were downregulated after hemin treatment. Moreover, to improve medication adherence, hemin was further formulated into the *in-situ* forming implant (hemin-ISFI). A single injection of the hemin-ISFI attained sustained remission of RA for at least six weeks. The ultra-long-acting hemin-ISFI decreased the total dose of hemin by nearly two-thirds, improving the safety and adherence. Overall, once-monthly hemin-ISFI injection potentially maximizes clinical benefits at a minimal dose, and holds great promise for rapid clinical translation in the treatment of RA via strong anti-inflammatory and immunosuppressive actions.

RESULTS

Prophylactic effects of hemin in the AIA model

Clinically, early pharmacological interventions could delay or even prevent the onset of RA in patients who have pre-rheumatoid arthritis features, such as swollen joints, but do not meet criteria for RA (Burmester and Pope, 2017). It has been reported that in the cellular defense against oxidative and inflammatory processes, the stress-responsive enzyme HO-1 plays a pivotal role (Loboda et al., 2016; Konrad et al., 2016). Thus, we hypothesized that the natural substrate for HO-1, hemin, may be repurposed for the treatment of RA. To test this hypothesis, we evaluated the prophylactic effects of hemin on acute inflammation and RA onset in the AIA model, which is one of the most widely used animal models of RA and provides the opportunity to study the severity of initial inflammation (Mossiat et al., 2015). AIA was established in rats and treatment with hemin was started 1 h before adjuvant immunization, as shown in Figure 1A. Changes of right hind paw thickness were measured every other day, and arthritis severity was assessed using the standardized clinical composite scores. The untreated AIA rats showed a rapid augmentation of paw thickness, and the paw swelling peaked at 24–48 h after immunization. At 24 h, the thickness change was more than 2.38 mm and the clinical score was up to four. Firstly, the effects of different doses and routes of administration on treatment efficacy were investigated. Administration of 40 mg/kg or 90 mg/kg of hemin (*i.p.*) resulted in efficiently reduced paw swelling, and no additional benefit was shown in hemin-treated rats given a dose of 90 mg/kg (Figures 1B, 1C, and S1A). Thus, a dose of 40 mg/kg of hemin was administered to evaluate the efficacy of treatment. In addition, *s.c.* injection did not compromise the anti-arthritic efficacy of hemin (Figures S1B and S1C). Strikingly, the AIA rats treated with hemin exhibited little paw thickening without developing a swelling peak, which was even superior to the efficacy of treatment with dexamethasone. Changes of thickness were maintained at less than 1 mm with a low clinical score (one to two) over a four-week period (Figures 1D–1G and S1D). In contrast, methotrexate and celecoxib did not confer protection from arthritis under identical conditions (Figures S1E, S1F, and S2). Together, hemin had a potent ability to suppress arthritis flares and thus prevented RA onset.

Therapeutic efficacy of hemin in the established CIA model

Given the significant prophylactic effects of hemin on RA onset, we next evaluated the therapeutic efficacy of hemin against established RA in the CIA model. CIA is the archetypical model of RA induced by active immunization and considered the most successful by evaluating therapeutic compounds both intra-articularly and systemically (Caplazi et al., 2015). CIA rats were injected with hemin (*i.p.*) twice weekly for two weeks at an optimal dose of 40 mg/kg (Figure 2A). Methotrexate (a disease modifying antirheumatic drug), dexamethasone (a corticosteroid), and celecoxib (a non-steroidal anti-inflammatory drug), which are three general classes of drugs commonly used in the treatment of RA, were also administered as controls. Figure 2 showed the progression of arthritis during the treatment period in terms of paw swelling and clinical score. Interestingly, a dramatic reduction in the paw swelling was observed in the hemin-treated group as early as 24 h after the start of treatment, compared with untreated CIA rats (Figure 2B). The efficacy of hemin treatment was comparable to dexamethasone which possesses strong anti-inflammatory effects (Figures 2C and S3). Moreover, compared with the celecoxib-treated or methotrexate-treated group, a significant decrease in clinical scores in the hemin-treated group was apparent throughout most of the treatment period (Figure 2D). The thickness changes of inflamed paws in CIA rats treated with hemin decreased from 1.98 ± 0.14 mm before treatment to 0.85 ± 0.30 mm after receiving six

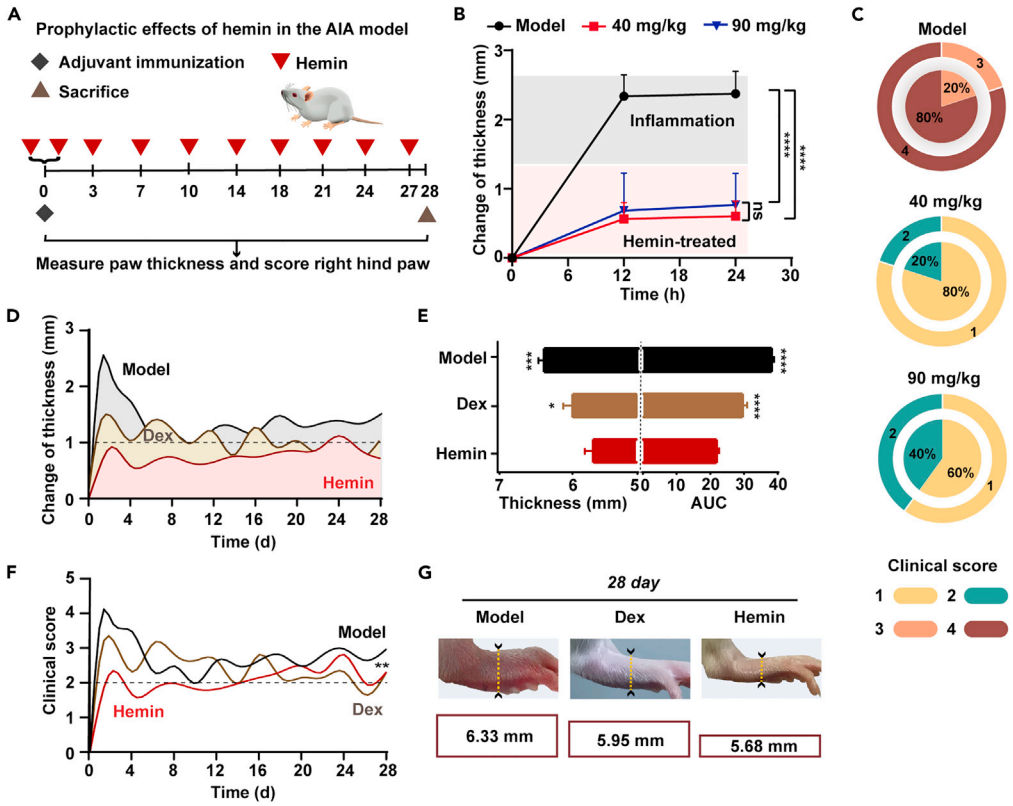

Figure 1. Prophylactic effects of hemin in AIA rats

(A) Experimental schedule of AIA establishment and treatment. Adjuvant immunization was given at day 0. Rats were treated with hemin (*i.p.*) from day 0 (1 h before immunization) twice weekly and sacrificed at day 28.

(B) Changes of hind paw thickness, and (C) clinical scores of AIA rats treated with hemin (*i.p.*, twice weekly) at 40 mg/kg or 90 mg/kg.

(D–F) (D) Changes of hind paw thickness, (E) the area under changes in paw thickness-time curve ($AUC_{0\text{-}28d}$), and (F) clinical scores of AIA rats given different treatments were compared with those of untreated AIA rats.

(G) Representative photographs of hind paws of AIA rats treated with hemin and dexamethasone (Dex) as controls at 24 h after immunization. Rats were administered with hemin (40mg/kg, *i.p.*, twice weekly), Dex (0.225 mg/kg, *i.m.*, twice weekly).

Data shown are mean ± SD ($n = 6$). (ns, no significance, *p < 0.05, **p < 0.01, ***p < 0.001, ****p < 0.0001). See also Figures S1 and S2.

consecutive injections, suggesting that less intense inflammatory reaction occurred after hemin treatment (Figure 2C). Whereas, untreated CIA rats showed continued progress in arthritis severity. Immunohistochemical analysis in inflamed joint tissue sections from CIA rats revealed that hemin treatment led to a markedly reduced production of the key proinflammatory cytokines TNFα, IL-6 and IL-17 (Figure 2E). By contrast, the expression level of FoxP3, a transcription factor directly linked to the immunosuppressive activity, was found to elevate compared with untreated CIA rats (Figure 2E). In addition, the arthritis activity in methotrexate-treated or celecoxib-treated rats remained severe, with the thickness change reaching 2 mm and the clinical scores close to that of untreated CIA rats (Figures 2B and 2D). These results demonstrated that hemin dramatically attenuated inflammatory response, resulting in marked amelioration of clinical course of established RA in CIA rats.

Hemin rescues dysregulated gene expression in RA rats

After establishing that hemin prevented the onset and ameliorated the clinical course of RA in both AIA and CIA models, we next turned to gain further insight into whether hemin treatment could rescue the dysregulated genes of RA. To address this issue, we attempted to map the possible immunological consequences of hemin treatment which may contribute to the amelioration of arthritis by RNA-seq. As hemin mainly accumulates in the liver after injection (Siegert and Holt, 2008), we chose the liver as the primary

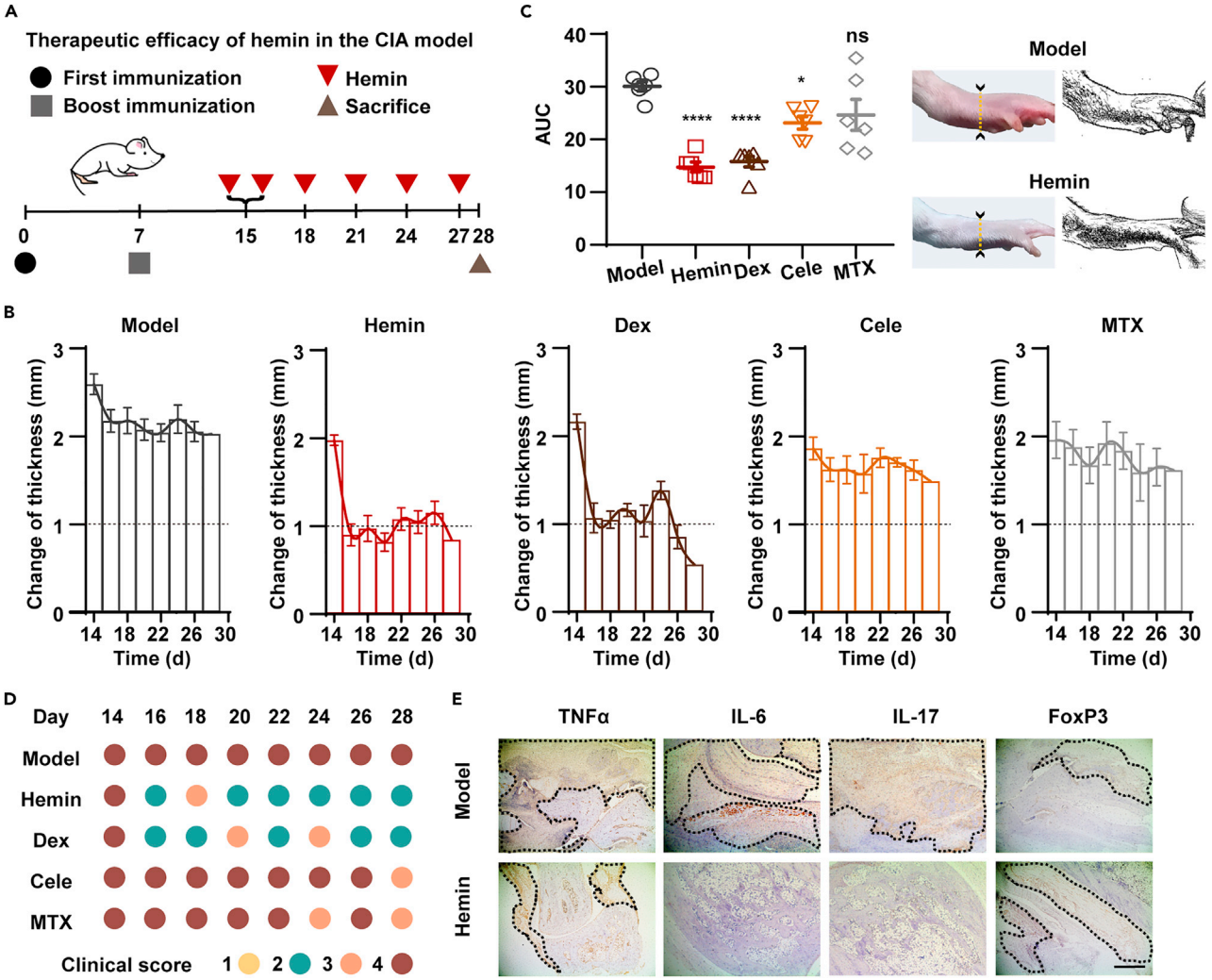

Figure 2. Therapeutic efficacy of hemin in CIA rats

(A) Experimental schedule of CIA establishment and treatment. The first immunization was given at day 0. Rats were treated with hemin (40 mg/kg, *i.p.*) from day 15 twice weekly and sacrificed at day 28.

(B) Changes of hind paw thickness of treated and untreated CIA rats.

(C) AUC of paw thickness change of CIA rats, and representative photographs of hind paws of hemin-treated CIA rats at day 28 after immunization.

(D) Clinical scores of treated CIA rats were compared with those of untreated CIA rats. Rats were treated with hemin (40 mg/kg, *i.p.*, twice weekly), Dex (0.45 mg/kg, *i.m.*, twice weekly), Cele (50 mg/kg, *i.g.*, twice weekly) and MTX (1 mg/kg, *i.p.*, twice weekly).

(E) Sections of inflamed joints were analyzed by immunohistochemical staining with anti- TNFα antibody, IL-6 antibody, IL-17 antibody or anti-FoxP3 antibody. Joint tissue sections were obtained from untreated and hemin-treated CIA rats. Scale bar, 500 μm.

Data shown are mean ± SD ($n = 6$). (ns, no significance, *$p < 0.05$, ****$p < 0.0001$). See also Figure S3.

target organ of hemin to assess its potential immunoregulatory effects. We defined the altered expression of 789 genes in the untreated RA group compared with the healthy group (Healthy *vs.* RA). And a total of 1,395 genes were differentially expressed in the hemin-treated group compared with the untreated RA group (RA *vs.* Treated). Notably, up to ~37% of the differentially expressed genes (DEGs) in the untreated RA group (295 genes) overlapped with those identified in the hemin-treated group (Figure 3A), indicating that hemin had a profound impact on the biological responses to RA. Dysregulated expression of 213 genes among the 295 overlapping DEGs was corrected by hemin. We then conducted the hierarchical clustering of these 213 DEGs in the untreated RA group and visualized using the heatmap. In the hemin-treated group, ~82% of 158 DEGs induced by inflammation were downregulated to an expression level close to that in the healthy group (Figure 3B). In addition, we assessed gene expression of immunoglobulin heavy constant gamma 1 (*Ighg1*), encoding the IgG class antibody heavy chain constant region, in paw tissues of

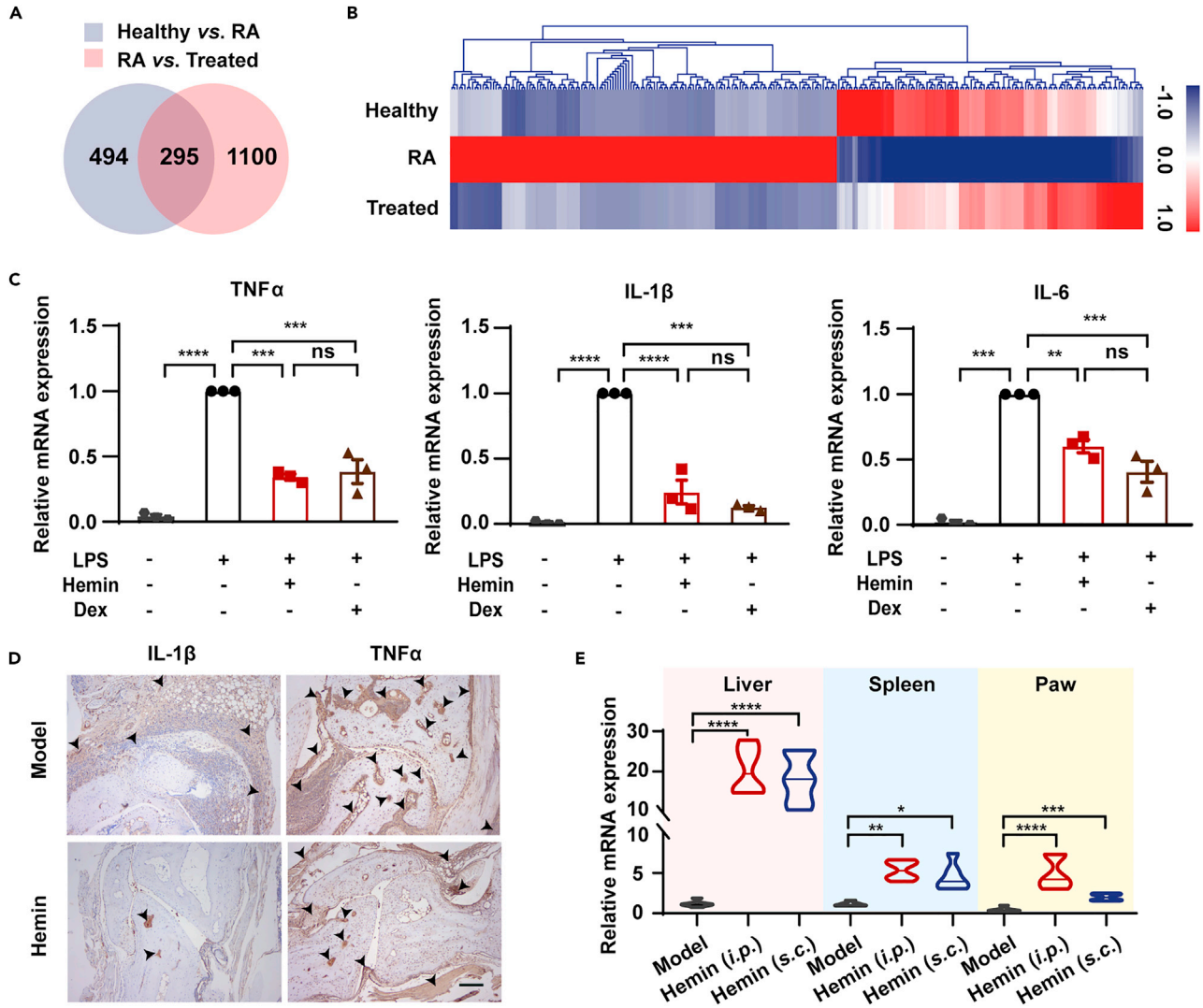

Figure 3. Hemin rescued the dysregulated gene expression in RA

(A) Venn diagram of differentially expressed genes (DEGs) in the untreated RA group compared with the healthy group (Healthy *vs.* RA) and the hemin-treated group compared with the RA group (RA *vs.* Treated).

(B) Heatmap derived from the hierarchical clustering of the representative 268 overlapping DEGs regulated by hemin. The dysregulated genes in the RA group were mostly corrected by hemin.

(C) Hemin inhibited the mRNA levels of proinflammatory cytokines in LPS-stimulated RAW 264.7 macrophages. Cells were stimulated by 500 ng/ml LPS for 6 h and incubated with 60 μM hemin or 250 nM Dex for 16 h, and the mRNA expression levels of IL-6, IL-1β, and TNFα were evaluated by qPCR.

(D) Sections of inflamed joints were analyzed by immunohistochemical staining with anti-IL-1β antibody or anti-TNFα antibody. Joint tissue sections were obtained from untreated and hemin-treated CIA rats. Magnification, ×100. Joints of hemin-treated CIA rats showed marked reductions of IL-1β and TNFα production (black arrows).

(E) Hemin strongly induced the expression of HO-1 *in vivo*. Total RNA was extracted from the livers, spleens, and hind paw tissues of CIA rats at day 28 after the first immunization. The mRNA expression of HO-1 was quantified by qPCR.

Data shown are mean ± SD ($n = 6$). (ns, no significance, *$p < 0.05$, **$p < 0.01$, ***$p < 0.001$, ****$p < 0.0001$).

See also Figures S4–S6.

CIA rats. Gene expression of *Ighg1* was markedly increased following the established CIA rat model. This increase in *Ighg1* gene expression was significantly inhibited in the hemin-treated group, as shown in Figure S4, suggesting reduction of immune activation with hemin in RA.

Next, we further validated the anti-inflammatory effects of hemin in lipopolysaccharides (LPS) stimulated RAW 264.7 macrophages, a well-established cellular model for anti-inflammatory drug screening

(Xu et al., 2017). We showed that LPS markedly up-regulated the mRNA expression of proinflammatory cytokines. These proinflammatory markers, including TNFα, IL-1β, and IL-6, were dramatically inhibited by nearly 50–70%, after treatment with 60 μM hemin (Figure 3C). Immunohistochemical analysis in inflamed joint tissue sections from CIA rats further confirmed that the treatment of RA with hemin markedly reduced production of the proinflammatory cytokines TNFα, IL-1β, IL-6 and IL-17, compared with untreated CIA rats (Figures 3D and S5). Hemin possessed anti-inflammatory activity most likely because of it being the natural substrate for HO-1, which has potent anti-inflammatory properties. We verified that hemin indeed stimulated HO-1 mRNA expression significantly both *in vitro* and *in vivo* (Figures 3E and S6A). Additionally, the anti-inflammatory responses of hemin were consistent with the downregulation of proinflammatory transcripts (Tril, Tnfrsf14, and Inava) identified by RNA-seq analysis *in vivo* (Figure S6B). Therefore, these results demonstrated that hemin could rescue dysregulated gene expression in RA rats and restore homeostasis.

Suppression of autoreactive Th1/Th17 immune responses *in vivo*

Since prior work has identified a pathogenic role of autoimmune disorders in RA, we then performed gene ontology (GO) enrichment analysis of 167 DEGs in the hemin-treated group involved in the immune system process (GO: 0002376) (Figures 4A and S7). These immune-related genes were enriched in the GO biological processes such as response to stimulus, inflammatory response, immune effector process, positive regulation of immune system process, and the most enriched GO term was response to stimulus (GO: 0050896) (Figure 4A). We thus inspected the DEGs enriched in response to stimulus. The heatmap showed the inhibition of interferon-related transcripts (*Irf5*, *Irf7*, *Irgm*, *Ifit2*, and *Ifit3*), as well as genes associated with Th cell activation and recruitment (*Cd300lf*, *Selplg, IL-1α, and AIF1*) (Figure 4B). The altered gene expression profile of Th cells revealed by RNA-seq implied that the symptomatic and disease-modifying effects of hemin might be attributed to the regulation of autoreactive Th cells. A lineage of $CD4^+$ Th cells, Th1 cells, is well-recognized to drive inflammation in RA (Minamino et al., 2001). We therefore sought to validate whether hemin modulated the differentiation of Th1 cells in RA. Spleens of untreated CIA rats, hemin-treated CIA rats, and healthy rats were collected to analyze the proportions of $CD4^+IFN\text{-}\gamma^+$ Th1 cells using flow cytometry. The results indicated that the Th1 cell population was obviously increased by arthritis in untreated CIA rats, compared with healthy rats (Figure 4C). This supported that collagen immunization triggered a Th1-biased immune activation in established rat models of RA. Intriguingly, we found that the frequency of splenic Th1 cells was severely decreased in hemin-treated CIA rats and returned to normal levels as healthy rats, suggesting that hemin compromised the activated Th1 immune responses.

Emerging evidence detailed that Th17 is another critical initiator of RA (Dardalhon et al., 2008; Pfeifle et al., 2017). Local Th17 cells orchestrate tissue inflammation by inducing proinflammatory cytokines and chemokines, recruiting inflammatory cells, and then bolstering the inflammatory cascades (Komatsu et al., 2014; Hirota et al., 2018). Thus, we evaluated the mRNA expression of Th17-related cytokines in inflamed hind paw tissues of CIA rats using qPCR. As shown in Figure 4D, the mRNA expression levels of IL-6 and IL-23, which induce Th17 differentiation and expand the Th17 population (Minamino et al., 2001; Chemin et al., 2019), were significantly down-regulated in response to treatment with hemin, consistent with the inhibition of arthritis flares. Furthermore, decreased mRNA levels of IL-17 and IL-21, the proinflammatory cytokines primarily produced by Th17 cells (Baeten and Kuchroo, 2013; Bartlett et al., 2014), were further identified in hemin-treated CIA rats (Figures 4D and S8). These Th17-related cytokines were also inhibited by dexamethasone treatment, yet IL-23 and IL-21 were not affected by treatment with celecoxib or methotrexate. Overall, these results suggested that hemin could inhibit Th1/Th17 responses, resulting in the down-regulation of proinflammatory cytokines and suppression of autoimmune responses in RA.

Preparation and characterization of ultra-long-acting hemin-ISFI

To avoid frequent dosing and improve therapeutic adherence, we next formulated hemin into the ISFI (hemin-ISFI) to develop a long-acting injectable formulation. Hemin-ISFI was prepared by sufficiently mixing the PLGA matrix dissolved in N-methyl-2-pyrrolidone and hemin powder. To test the injectability, rheological analysis of hemin-ISFI was performed and the injectable blank implant matrix served as a control. The results showed that the viscosity of hemin-ISFI was higher than that of the blank PLGA matrix, likely because of the incorporation of suspending hemin powder. Importantly, hemin-ISFI exhibited non-Newtonian shear-thinning behavior and its viscosity gradually decreased under shear strain (Figures 5A and S9). The

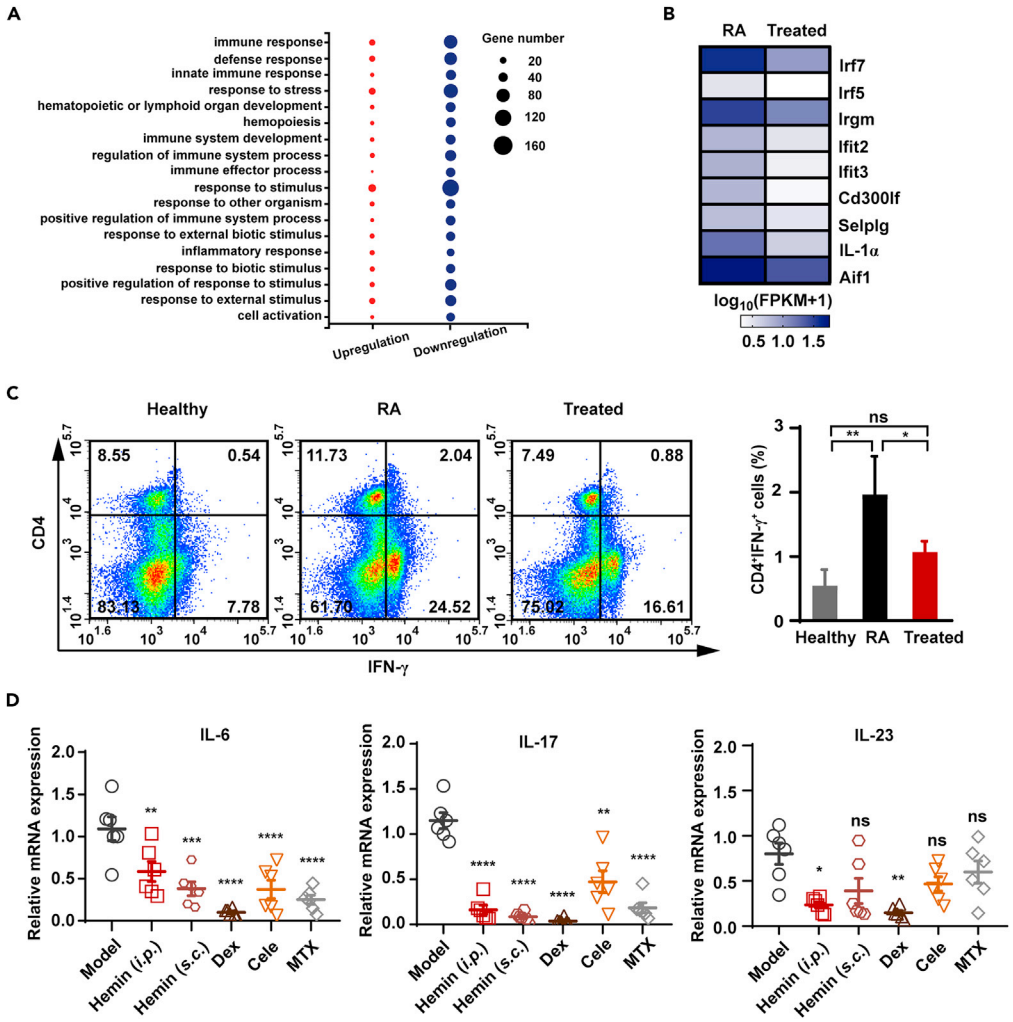

Figure 4. Hemin suppressed autoreactive Th1/Th17 responses *in vivo*

(A) GO enrichment analysis of 167 DEGs involved in the immune system process (GO:0002376) in the hemin-treated group.

(B) Heat map showing the $\log_{10}$ (FPKM+1) changes of Th1/Th17-related DEGs in the hemin-treated group enriched in response to stimulus (GO:0050896). *Irf7*, interferon regulatory factor 7; *Irf5*, interferon regulatory factor 5; *Irgm*, immunity related GTPase M; *Ifit2*, interferon induced protein with tetratricopeptide repeats 2; *Ifit3*, interferon induced protein with tetratricopeptide repeats 3; *Cd300lf*, CD300 molecule like family member f; *Selplg*, selectin P ligand; *Aif1*, allograft inflammatory factor 1.

(C) Flow cytometry analysis of splenic $CD4^+$ IFN-γ^+ Th1 cell proportion in healthy rats, untreated or hemin-treated CIA rats.

(D) Quantitative mRNA expression of Th17-related cytokines IL-6, IL-17, and IL-23 in inflamed hind paw tissues of treated CIA rats at day 28 after the first immunization.

Data shown are mean ± SD (n = 6). (ns, no significance, *p < 0.05, **p < 0.01, ***p < 0.001, ****p < 0.0001). See also Figures S7 and S8.

shear-thinning behavior of hemin-ISFI is suitable for the injection, because the viscosity near the injection well is lower due to higher shear rate, which provides more favorable injectability.

After being subcutaneously injected into RA rats, hemin-ISFI formed hydrogel with a porous sponge-like structure (Figure 5B). The hemin-ISFI could avoid surgical removal after the complete release of the payload because of their biodegradation. To verify the biodegradation of hemin-ISFI, we isolated the implants at day 10 and day 60 and measured their changes of dimensions and dry weights. The diameters and dry mass of the hemin-ISFI at day 60 were markedly reduced, compared with those at day 10 (Figures 5C

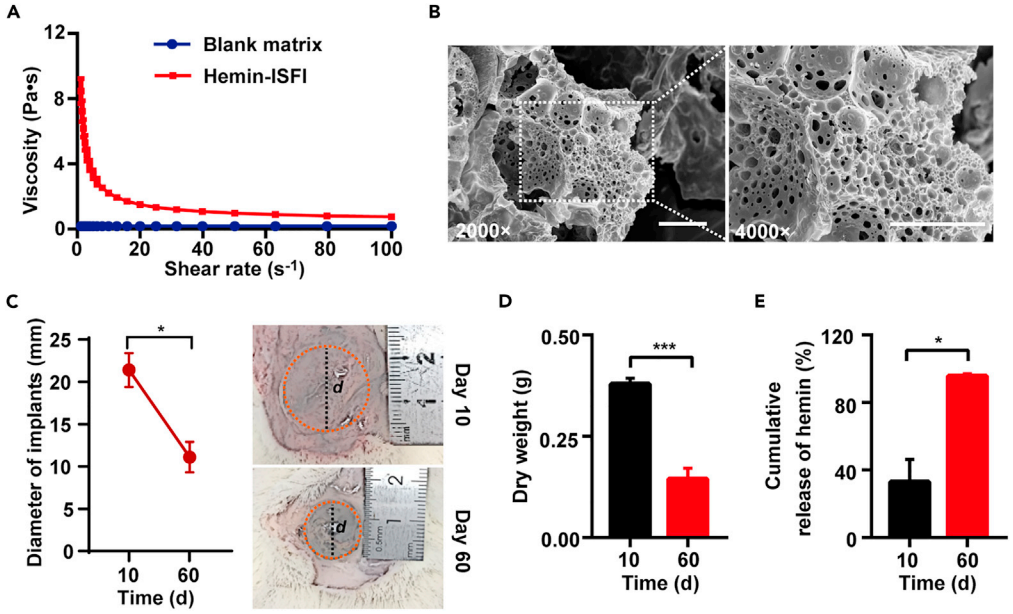

Figure 5. Characterization of ultra-long-acting hemin-ISFI

(A) Shear-thinning properties of hemin-ISFI. The viscosities of hemin-ISFI and blank matrix were measured by steady rate scanning.

(B) SEM images showed a sponge-like porous structure of hemin-ISFI harvested at day 10 after *s.c.* injection. Scale bar, 10 μm.

(C) Biodegradation of hemin-ISFI *in vivo*. Diameters (*d*) of the isolated implants shrank at day 60 compared with those at day 10 due to degradation of the polymer matrix.

(D) The dry weights of the lyophilized implants formed in hemin-ISFI-treated rats at day 10 and day 60.

(E) Cumulative release of hemin from the implants formed in hemin-ISFI-treated rats.

Data shown are mean ± SD ($n = 3$). (*$p < 0.05$, ***$p < 0.001$). See also Figure S9.

and 5D), demonstrating that hemin-ISFI was biodegradable. We then examined whether the slow degradation of these implant matrices led to the sustained-release of hemin over long periods. The contents of residual hemin in the implants were measured and the percentage of released hemin was determined by subtracting the residuals from total drug mass (Figure 5E). At day 10, 33.04% of the total drug was released from the implants. The released proportion increased to 95.74% at day 60, achieving almost complete release of the payload. Overall, these results demonstrated the promise of using the ISFI formulation as an ultra-long-acting hemin injection for improving therapeutic adherence.

Once-monthly long-acting hemin achieve sustained remission and joint protection in RA at least six weeks

Having determined that hemin-ISFI offered sustained-release of hemin for two months, we next evaluated whether it could achieve long-term remission in animal models of RA. AIA rats were treated with hemin-ISFI by *s.c.* injection at a dose of 120 mg/kg (Figure 6A). The results showed that a single injection of hemin-ISFI effectively prevented AIA onset for at least one month (Figures 6B, 6D, S10A, and S10B). Compared with the methotrexate-treated group, the hemin-ISFI-treated AIA rats exhibited very mild symptoms of inflammation, as well as a markedly lower clinical score during the four-week period of treatment. Furthermore, we treated CIA rats with hemin-ISFI (120 mg/kg, *s.c.*) at day 15 after the first immunization. Changes of hind paw thickness and clinical scores were measured every other day. The severe paw swelling and erythema were soon alleviated by the initial two doses of *i.p.* injection of hemin. Inspiringly, therapy with a single *s.c.* injection of hemin-ISFI achieved a long-term remission for at least six weeks and produced dramatic attenuation of the course of disease, as determined by reduction of swelling in the initially involved limb (Figures 6C, 6D, S10C, and S10D). The paw thickness changes in hemin-ISFI-treated CIA rats decreased from 1.82 ± 0.36 mm before treatment at day 14 to 1.08 ± 0.49 mm at day 56. Notably, by using hemin-ISFI, the total dose for two months was 200 mg/kg, which was markedly reduced by nearly two-thirds, compared with the cumulative dose of hemin given by *i.p.* injection (560 mg/kg). Taken together, these results suggested that

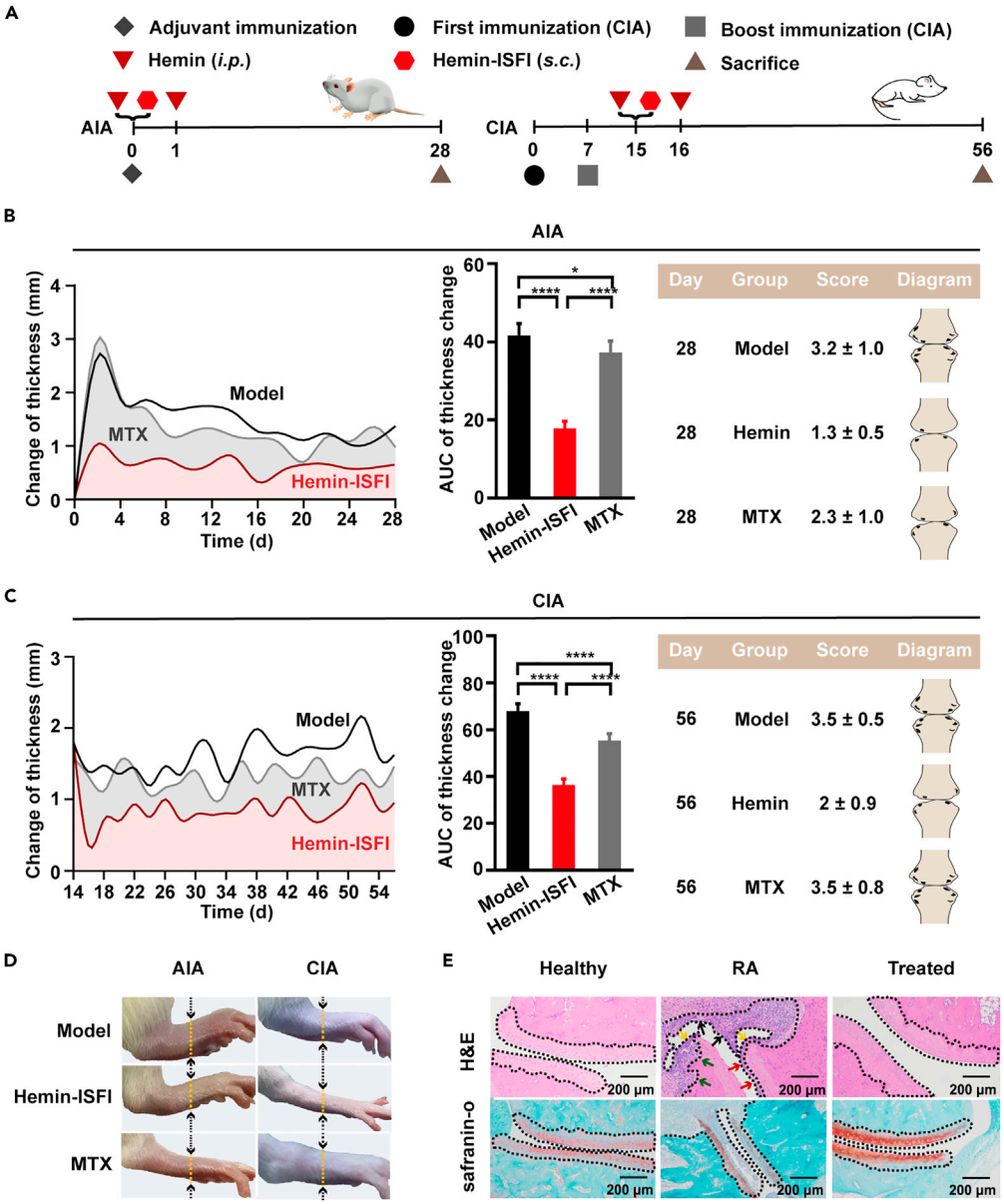

Figure 6. Monthly hemin-ISFI injection achieved long-acting symptomatic and disease-modifying effects in RA rats

(A) Experimental schedule of treating RA rats with hemin-ISFI. AIA rats were injected with hemin-ISFI (120 mg/kg, *s.c.*) at one hour before adjuvant at day 0. CIA rats were treated with hemin-ISFI (120 mg/kg, *s.c.*) on day 15 after the first immunization. Hemin-ISFI was administered combining two doses of *i.p.* injection of hemin (40 mg/kg/day) at the beginning of treatment.

(B) Changes of hind paw thickness, AUC of thickness change, and clinical scores of untreated AIA rats, hemin-ISFI-treated or MTX-treated AIA rats. Hemin-ISFI prevented the onset of RA for four weeks.

(C) Changes of hind paw thickness, AUC of thickness change, and clinical scores of untreated CIA rats, hemin-ISFI-treated or MTX-treated CIA rats. A single dose of hemin-ISFI achieved sustained remission for at least six weeks. Clinical severity scores of RA rats at day 28 (for AIA rats) or day 56 (for CIA rats) used to evaluate the therapeutic efficacy of hemin and MTX. Score 1: mild swelling confined to the tarsals of ankle joint; Score 2: ≥1 erosion, mild swelling extending from the ankle to the tarsals; Score 3: marked erosions, moderate swelling extending from the ankle to metatarsal joints; Score 4: sever erosions, severe swelling encompass the ankle, foot and digits, or ankylosis of the limb.

(D) Representative photographs of hind paws of untreated RA rats, hemin-ISFI-treated rats, and MTX-treated rats at day 28 (for AIA rats) or day 56 (for CIA rats).

Figure 6. *Continued*

(E) Representative H&E staining (upper panels) and safranin-o staining (lower panels) images (100×) of ankle joints isolated from healthy rats, untreated CIA rats, or hemin-ISFI treated rats at day 56. Inflammatory cell infiltration (black arrows and green arrows), synovial hypotrophy (black arrows), pannus formation (red arrows), and cartilage erosion (yellow arrows) were indicated in the images. Scale bar, 200 μm.

Data shown are mean ± SD ($n = 6$). (*$p < 0.05$, ****$p < 0.0001$). See also Figure S10.

once-monthly hemin-ISFI acted as an effective ultra-long-acting formulation with a remarkable dose reduction for preventing and curing RA.

The severity of synovitis and joint damage were then evaluated by histological analysis with safranin-o and H&E staining (Figure 6E). Ankle joints of hemin-ISFI-treated CIA rats, untreated CIA rats, and healthy rats were collected at day 56 after the first immunization. Joints of untreated CIA rats showed a massive influx of inflammatory cells with synovial hypotrophy (black arrows) and pannus formation (red arrows). The infiltrating cells eroded the cartilage layer (yellow arrows) and filled the marrow cavity (green arrows). The evident proteoglycan loss in damaged cartilage was further revealed by decreased intensity of safranin-o staining. In contrast, a representative ankle joint from hemin-ISFI-treated CIA rats manifested normal architecture with a normal synovial membrane and smooth cartilaginous surfaces indistinguishable from a normal joint. These results suggested that hemin-ISFI therapy could protect ankle joints against synovitis and cartilage erosion in RA.

DISCUSSION

Repurposing old drugs for new clinical indications may allow faster development, at reduced costs and possibly with fewer safety concerns, showing promise for difficult-to-treat diseases (Bertolini et al., 2015). The work presented in this study demonstrated that repurposing hemin, a drug originally approved for acute porphyria attacks as well as a natural substrate for HO-1, is a potential new weapon to treat RA that currently has no universally effective therapy. There are several advantages of hemin for RA treatment in animal models. First, hemin dramatically inhibited joint swelling within 24 h post-injection, and the symptoms of RA-related acute inflammation were almost completely suppressed by prophylactic and therapeutic treatment. This rapid onset of hemin is superior to that of methotrexate, the first-line drug for the treatment of RA. In patients receiving treatment with methotrexate, an appreciable time lag of several weeks occurs *in vivo* before a clinical benefit is seen (Brown et al., 2016). Moreover, hemin exerted both anti-inflammatory and immunosuppressive effects as glucocorticoids did, and prevented joint destruction in the RA models. The combination of low-dose glucocorticoids and methotrexate is used in clinical treatment for remission of RA (Verschueren et al., 2017; Stouten et al., 2018). Using glucocorticoids, however, risks impairing bone quality, which may aggravate arthritis severity (Hardy et al., 2020). In the CIA model, hemin had no adverse effect of osteoporosis, as shown by histological analysis. Thus, these findings provided persuasive evidence that repurposing hemin may be an effective inspiring approach to the treatment of RA.

RA is a multifactorial disease with multiple effects following immune activation such as synovial membrane inflammation, cartilage damage, and bone erosion (Guo et al., 2018). The restoration of immune homeostasis at the transcriptomic level may explain the robust anti-arthritic effects of hemin. RNA-seq analysis showing regulated expression of Th cell-related genes hinted that hemin exerted immunosuppressive effects on $CD4^+$ Th cells. $CD4^+$ Th cells are central in initiating and perpetuating the chronic autoimmune response (Skapenko et al., 2005). The Th1 subset of $CD4^+$ Th cells secretes IFN-γ and other Th1 cytokines associated with inflammation, and promotes cell-mediated immune responses (Arbore et al., 2016). The clinical observation indicates that the marked decrease in Th1-mediated immunity during pregnancy improves the symptoms of RA and enables these pregnant patients to taper or even stop the use of medications (Da Silva and Spector, 1992). In the present study, we unraveled that hemin could regulate pathogenic $CD4^+$ Th cells by decreasing splenic $CD4^+IFN\text{-}\gamma^+$ Th1 cell proportion to treat RA efficiently in animal models. On the other hand, we noticed that hemin significantly down-regulated mRNA expression of Th17-inducing cytokines such as IL-6, IL-23, and IL-21, as well as Th17-secreted IL-17. Emerging evidence suggests that Th17 cells, another critical initiator in RA, amplify inflammatory cascades (Dardalhon et al., 2008; Nistala et al., 2010). Synovial Th17 cells augment chronic joint inflammation by recruiting neutrophils, activating fibroblast-like synoviocytes, and inducing bone resorption (Hirota et al., 2018; Chemin et al., 2019). Thus, the down-regulation of Th17-related cytokine profiles in the hemin-treated group antagonized synovitis and cartilage erosion in the CIA model, as shown by the histological analysis of ankle joints. The

Th17 subset of $CD4^+$ T cells are important in the pathogenesis of inflammatory disease, but the mechanisms of their actions and the role of the development of Th1 cells are incompletely understood. The precise molecular mechanisms underlying the anti-arthritic effects of hemin in the treatment of RA will be extensively explored in our future work. In addition, it should be noted that the CIA and AIA animal models used in the present study and other preclinical studies of RA represent aspects of human RA, but have also limitations in recapitulating the pathogenetic spectrum and predicting treatment effects in human RA. Thereby, a better understanding of the molecular mechanisms of hemin and proving the efficacy in treating human RA will pave the way for promising treatment options for RA patients.

RA is a chronic and progressive disease that requires long-term therapy. However, the full clinical benefits of the RA treatment are often attenuated because patients do not take their medications as prescribed timing or dose (Marengo and Suarez-Almazor, 2015). In this study, an optimal dose of 40 mg/kg of hemin was injected consecutively to maintain its anti-arthritic effects. Clinically, hemin is administered by daily *i.v.* injection for the treatment of acute porphyria attacks. Such frequent administration would cause poor adherence to the long-term RA therapies, and compromise the effectiveness of treatment. To improve medication adherence, we further formulated hemin into the long-acting *in-situ* forming implant. The results presented that once-monthly injection of hemin-ISFI achieved sustained remission of RA for at least six weeks. The dose of hemin-ISFI was decreased to only one-third of the cumulative dose of hemin *i.p.* injection, significantly improving safety and adherence. The favorable long-acting efficacy was attributed to the subcutaneous drug depot formed by the biocompatible polymer matrix PLGA (Jain et al., 2016). PLGA underwent a phase inversion and precipitated to form a hydrogel network after contacting body fluids, which allowed the prolonged release of the drug, and favored dose reduction, as well as avoided frequent administration (Benhabbour et al., 2019; Parent et al., 2013). Thus, the once-monthly hemin-ISFI injection holds great promise for bringing good therapeutic adherence to RA patients.

In summary, this study demonstrated that hemin, a drug prescribed for patients with attacks of acute porphyria, prevented the onset and ameliorated the course of RA in animal models via anti-inflammatory and immunosuppressive actions. The potent immunoregulatory effects of hemin on pathogenic Th1/Th17 responses laid the groundwork for further investigating the causal link between its immunosuppression and therapeutic benefits. We further developed a once-monthly ultra-long-acting hemin-ISFI with good medication adherence. A single *s.c.* injection of the hemin-ISFI efficiently inhibited joint swelling and protected against joint damage for at least six weeks at a relatively low dose. Thus, teaching hemin with new tricks and formulating it into a once-monthly long-acting injection provided a promising strategy for improving clinical outcomes in treating RA, and possibly other autoimmune diseases.

Limitations of the study

We developed a once-monthly hemin injection as a repurposed therapy in animal models of RA via anti-inflammatory and immunosuppressive actions. But the molecular mechanisms underlying the anti-rheumatoid arthritis effects of hemin need to be further explored. In addition, comparing the effectiveness of hemin *vs* approved biological or synthetic DMARDs, and the limitations of the AIA and CIA animal models in predicting clinical efficacy of treatments in human RA need to be explored through further research.

STAR★METHODS

Detailed methods are provided in the online version of this paper and include the following:

- KEY RESOURCES TABLE
- RESOURCE AVAILABILITY
  - Lead contact
  - Materials availability
  - Data and code availability
- EXPERIMENTAL MODELS AND SUBJECT DETAILS
  - Animal studies
  - Cell line
  - Primary cells
- METHOD DETAILS
  - Evaluation of prophylactic effects of hemin in the AIA model
  - Determination of therapeutic efficacy of hemin in the CIA model

- RNA sequencing
- *In vitro* inhibition of proinflammatory cytokines and induction of HO-1
- RNA preparation and qPCR analysis
- Flow cytometry analysis
- Preparation and characterization of the long-acting hemin-ISFI
- Investigation of long-acting anti-arthritic effects of hemin-ISFI
- Histological analysis of ankle joints

● QUANTIFICATION AND STATISTICAL ANALYSIS

SUPPLEMENTAL INFORMATION

Supplemental information can be found online at https://doi.org/10.1016/j.isci.2021.103101.

ACKNOWLEDGMENTS

The work was supported by the National Natural Science Foundation of China (Project No. 82073771), the Science and Technology Foundation of Guangzhou (Project No.201904010425), Guangdong Provincial Key Laboratory of Chiral Molecule and Drug Discovery (Project No. 2019B030301005), Natural Science Foundation of Guangdong Province (Project No. 2021A1515011593), the 2020 Guangdong Provincial Science and Technology Innovation Strategy Special Fund (Guangdong-Hong Kong-Macau Joint Lab) (Project No. 2020B1212030006)

AUTHOR CONTRIBUTIONS

B.S. and G.L. conducted the experiments. B.S and L.G. analyzed the data. B.S. and L.G. and M.F. wrote the manuscript. R.H. and M.F. conceived the project. All authors discussed the results and gave final approval of the manuscript.

DECLARATION OF INTERESTS

The authors declare no competing financial interests.

INCLUSION AND DIVERSITY

We worked to ensure sex balance in the selection of non-human subjects. We worked to ensure diversity in experimental samples through the selection of the cell lines. We worked to ensure diversity in experimental samples through the selection of the genomic datasets. While citing references scientifically relevant for this work, we also actively worked to promote gender balance in our reference list.

Received: May 17, 2021
Revised: September 3, 2021
Accepted: September 3, 2021
Published: October 22, 2021

REFERENCES

Arbore, G., West, E.E., Spolski, R., Robertson, A.A.B., Klos, A., Rheinheimer, C., Dutow, P., Woodruff, T.M., Yu, Z.X., O'Neill, L.A., et al. (2016). T helper 1 immunity requires complement-driven NLRP3 inflammasome activity in CD4(+) T cells. Science *352*, aad1210.

Baeten, D., and Kuchroo, V.K. (2013). How cytokine networks fuel inflammation: Interleukin-17 and a tale of two autoimmune diseases. Nat. Med. *19*, 824–825.

Bartlett, H.S., and Million, R.P. (2014). Targeting the IL-17-T(H)17 pathway. Nat. Rev. Drug Discov. *14*, 11–12.

Benhabbour, S.R., Kovarova, M., Jones, C., Copeland, D.J., Shrivastava, R., Swanson, M.D., Sykes, C., Ho, P.T., Cottrell, M.L., Sridharan, A., et al. (2019). Ultra-long-acting tunable biodegradable and removable controlled release implants for drug delivery. Nat. Commun. *10*, 4324.

Bertolini, F., Sukhatme, V.P., and Bouche, G. (2015). Drug repurposing in oncology—patient and health systems opportunities. Nat. Rev. Clin. Oncol. *12*, 732–742.

Brand, D.D., Latham, K.A., and Rosloniec, E.F. (2007). Collagen-induced arthritis. Nat. Protoc. *2*, 1269–1275.

Brown, P.M., Pratt, A.G., and Isaacs, J.D. (2016). Mechanism of action of methotrexate in rheumatoid arthritis, and the search for biomarkers. Nat. Rev. Rheumatol. *12*, 731–742.

Burmester, G.R., and Pope, J.E. (2017). Novel treatment strategies in rheumatoid arthritis. Lancet *389*, 2338–2348.

Caplazi, P., Baca, M., Barck, K., Carano, R.A., DeVoss, J., Lee, W.P., Bolon, B., and Diehl, L. (2015). Mouse models of rheumatoid arthritis. Vet. Pathol. *52*, 819–826.

Chemin, K., Gerstner, C., and Malmstrom, V. (2019). Effector functions of CD4+ T cells at the site of local autoimmune inflammation—lessons from rheumatoid arthritis. Front. Immunol. *10*, 353.

Da Silva, J.A.P., and Spector, T.D. (1992). The role of pregnancy in the course and aetiology of rheumatoid arthritis. Clin. Rheumatol. *11*, 189–194.

Dardalhon, V., Korn, T., Kuchroo, V.K., and Anderson, A.C. (2008). Role of Th1 and Th17 cells in organ-specific autoimmunity. J. Autoimmun. *31*, 252–256.

Devesa, I., Ferrándiz, M.L., Terencio, M.C., Joosten, L.A.B., Berg, W.B.V.D., and Alcaraz, M.J. (2005). Influence of heme oxygenase 1 modulation on the progression of murine collagen-induced arthritis. Arthritis Rheum. *52*, 3230–3238.

Eberhardt, K., Larsson, B.M., Nived, K., and Lindqvist, E. (2007). Work disability in rheumatoid arthritis—development over 15 years and evaluation of predictive factors over time. J. Rheumatol. *34*, 481–487.

Ferrandiz, M.L., Maicas, N., Garcia-Arnandis, I., Terencio, M.C., Motterlini, R., Devesa, I., Joosten, L.A., van den Berg, W.B., and Alcaraz, M.J. (2008). Treatment with a CO-releasing molecule (CORM-3) reduces joint inflammation and erosion in murine collagen-induced arthritis. Ann. Rheum. Dis. *67*, 1211–1217.

Ferrara, G., Mastrangelo, G., Barone, P., La Torre, F., Martino, S., Pappagallo, G., Ravelli, A., Taddio, A., Zulian, F., Cimaz, R., et al. (2018). Methotrexate in juvenile idiopathic arthritis: advice and recommendations from the MARAJIA expert consensus meeting. Pediatr. Rheumatol. Online J. *16*, 46.

Fraenkel, L., Bathon, J.M., England, B.R., St Clair, E.W., Arayssi, T., Carandang, K., Deane, K.D., Genovese, M., Huston, K.K., Kerr, G., et al. (2021). 2021 American college of rheumatology guideline for the treatment of rheumatoid arthriti. Arthritis Rheumatol. *73*, 1108–1123.

Guo, Q., Wang, Y., Xu, D., Nossent, J., Pavlos, N.J., and Xu, J. (2018). Rheumatoid arthritis: pathological mechanisms and modern pharmacologic therapies. Bone Res. *6*, 15.

Hardy, R.S., Raza, K., and Cooper, M.S. (2020). Therapeutic glucocorticoids: mechanisms of actions in rheumatic diseases. Nat. Rev. Rheumatol. *16*, 133–144.

Hirota, K., Hashimoto, M., Ito, Y., Matsuura, M., Ito, H., Tanaka, M., Watanabe, H., Kondoh, G., Tanaka, A., Yasuda, K., et al. (2018). Autoimmune Th17 cells induced synovial stromal and innate lymphoid cell secretion of the cytokine GM-CSF to initiate and augment autoimmune arthritis. Immunity *48*, 1220–1232.e25.

Ho, C.T.K., Mok, C.C., Cheung, T.T., Kwok, K.Y., and Yip, R.M.L. (2019). Management of rheumatoid arthritis: 2019 updated consensus recommendations from the Hong Kong Society of Rheumatology. Clin. Rheumatol. *38*, 1–20.

Jain, A., Kunduru, K.R., Basu, A., Mizrahi, B., Domb, A.J., and Khan, W. (2016). Injectable formulations of poly(lactic acid) and its copolymers in clinical use. Adv. Drug Deliv. Rev. *107*, 213–227.

Kitamura, A., Nishida, K., Komiyama, T., Doi, H., Kadota, Y., Yoshida, A., and Ozaki, T. (2011). Increased level of heme oxygenase-1 in rheumatoid arthritis synovial fluid. Mod. Rheumatol. *21*, 150–157.

Kobayashi, H., Takeno, M., Saito, T., Takeda, Y., Kirino, Y., Noyori, K., Hayashi, T., Ueda, A., and Ishigatsubo, Y. (2006). Regulatory role of heme oxygenase 1 in inflammation of rheumatoid arthritis. Arthritis Rheum. *54*, 1132–1142.

Komatsu, N., Okamoto, K., Sawa, S., Nakashima, T., Oh-Hora, M., Kodama, T., Tanaka, S., Bluestone, J.A., and Takayanagi, H. (2014). Pathogenic conversion of Foxp3+ T cells into TH17 cells in autoimmune arthritis. Nat. Med. *20*, 62–68.

Konrad, F.M., Knausberg, U., Hone, R., Ngamsri, K.C., and Reutershan, J. (2016). Tissue heme oxygenase-1 exerts anti-inflammatory effects on LPS-induced pulmonary inflammation. Mucosal Immunol. *9*, 98–111.

Liang, H., Peng, B., Dong, C., Liu, L., Mao, J., Wei, S., Wang, X., Xu, H., Shen, J., and Mao, H.Q. (2018). Cationic nanoparticle as an inhibitor of cell-free DNA-induced inflammation. Nat. Commun. *9*, 4291.

Loboda, A., Damulewicz, M., Pyza, E., Jozkowicz, A., and Dulak, J. (2016). Role of Nrf2/HO-1 system in development, oxidative stress response and diseases: an evolutionarily conserved mechanism. Cell. Mol. Life Sci. *73*, 3221–3247.

Marengo, M.F., and Suarez-Almazor, M.E. (2015). Improving treatment adherence in patients with rheumatoid arthritis: what are the options? Int. J. Clin. Rheumtol. *10*, 345–356.

Minamino, T., Christou, H., Hsieh, C.M., Liu, Y., Dhawan, V., Abraham, N.G., Perrella, M.A., Mitsialis, S.A., and Kourembanas, S. (2001). Targeted expression of heme oxygenase-1 prevents the pulmonary inflammatory and vascular responses to hypoxia. Proc. Natl. Acad. Sci. U S A *98*, 8798–8803.

Moon, S.J., Kim, E.K., Jhun, J.Y., Lee, H.J., Lee, W.S., Park, S.H., Cho, M.L., and Min, J.K. (2017). The active metabolite of leflunomide, A77 1726, attenuates inflammatory arthritis in mice with spontaneous arthritis via induction of heme oxygenase-1. J. Transl. Med. *15*, 31.

Mossiat, C., Laroche, D., Prati, C., Pozzo, T., Demougeot, C., and Marie, C. (2015). Association between arthritis score at the onset of the disease and long-term locomotor outcome in adjuvant-induced arthritis in rats. Arthritis Res. Ther. *17*, 184.

Nair, N., Plant, D., Verstappen, S.M., Isaacs, J.D., Morgan, A.W., Hyrich, K.L., Barton, A., and Wilson, A.G. (2020). Differential DNA methylation correlates with response to methotrexate in rheumatoid arthritis. Rheumatology *59*, 1364–1371.

Nistala, K., Adams, S., Cambrook, H., Ursu, S., Olivito, B., de Jager, W., Evans, J.G., Cimaz, R., Bajaj-Elliott, M., and Wedderburn, L.R. (2010). Th17 plasticity in human autoimmune arthritis is driven by the inflammatory environment. Proc. Natl. Acad. Sci. U S A *107*, 14751–14756.

Parent, M., Nouvel, C., Koerber, M., Sapin, A., Maincent, P., and Boudier, A. (2013). PLGA in situ implants formed by phase inversion: critical physicochemical parameters to modulate drug release. J. Contr. Release *172*, 292–304.

Pfeifle, R., Rothe, T., Ipseiz, N., Scherer, H.U., Culemann, S., Harre, U., Ackermann, J.A., Seefried, M., Kleyer, A., Uderhardt, S., et al. (2017). Regulation of autoantibody activity by the IL-23-TH17 axis determines the onset of autoimmune disease. Nat. Immunol. *18*, 104–113.

Siegert, S.W., and Holt, R.J. (2008). Physicochemical properties, pharmacokinetics, and pharmacodynamics of intravenous hematin: a literature review. Adv. Ther. *25*, 842–857.

Skapenko, A., Leipe, J., Lipsky, P.E., and Schulze-Koops, H. (2005). The role of the T cell in autoimmune inflammation. Arthritis Res. Ther. *7*, S4.

Smolen, J.S., Aletaha, D., and McInnes, I.B. (2016). Rheumatoid arthritis. Lancet *388*, 2023–2038.

Stouten, V., Joly, J., Pazmino, S., Van der Elst, K., De Cock, D., Westhovens, R., and Verschueren, P. (2018). OP0034 Long-term effectiveness of the cobra slim remission induction and treat to target strategy in patients with early rheumatoid arthritis lacking classical markers of poor prognosis: 2 year results of the carera trial. Ann. Rheum. Dis. *77*, 67.

Verschueren, P., De Cock, D., Corluy, L., Joos, R., Langenaken, C., Taelman, V., Raeman, F., Ravelingien, I., Vandevyvere, K., Lenaerts, J., et al. (2017). Effectiveness of methotrexate with step-down glucocorticoid remission induction (COBRA Slim) versus other intensive treatment strategies for early rheumatoid arthritis in a treat-to-target approach: 1-year results of CareRA, a randomised pragmatic open-label superiority trial. Ann. Rheum. Dis. *76*, 511–520.

Wruck, C.J., Fragoulis, A., Gurzynski, A., Brandenburg, L.O., Kan, Y.W., Chan, K., Hassenpflug, J., Freitag-Wolf, S., Varoga, D., Lippross, S., et al. (2011). Role of oxidative stress in rheumatoid arthritis: insights from the Nrf2-knockout mice. Ann. Rheum. Dis. *70*, 844–850.

Xu, Q., Liu, M., Liu, Q., Wang, W., Du, Y., and Yin, H. (2017). The inhibition of LPS-induced inflammation in RAW264.7 macrophages via the PI3K/Akt pathway by highly N-acetylated chitooligosaccharide. Carbohydr. Polym. *174*, 1138–1143.

Yang, S., Ohe, R., Aung, N.Y., Kato, T., Kabasawa, T., Utsunomiya, A., Takakubo, Y., Takagi, M., and Yamakawa, M. (2019). Comparative study of HO-1 expressing synovial lining cells between RA and OA. Mod. Rheumatol. *3*, 1–8.

Yang, Y., Zhang, X., Xu, M., Wu, X., Zhao, F., and Zhao, C. (2018). Quercetin attenuates collagen-induced arthritis by restoration of Th17/Treg balance and activation of heme oxygenase 1-mediated anti-inflammatory effect. Int. Immunopharmacol. *54*, 153–162.

STAR★METHODS

KEY RESOURCES TABLE

Reagent or RESOURCE	Source	Identifier
Antibodies		
APC Mouse Anti-Rat CD4	BD Biosciences	550057
FITC Mouse Anti-Rat IFN-γ	BD Biosciences	559498
Anti-Rat TNFα	Servicebio	GB13452
Anti-Rat IL-1β	Servicebio	GB11113
Anti-Rat IL-6	Servicebio	GB11117
Anti-Rat IL-17	Servicebio	GB11110
Anti-Rat Foxp3	Servicebio	GB11093
Chemicals, peptides, and recombinant proteins		
Hemin	Macklin Biochemical Technology	H811002; CAS: 16009-13-5
Celecoxib	Macklin Biochemical Technology	C830895; CAS: 169590-42-5
Dexamethasone 21-acetate	Macklin Biochemical Technology	D806496; CAS: 169590-42-5
Methotrexate	Macklin Biochemical Technology	M813626; CAS: 59-05-2
Sodium hydroxide	Zhiyuan Chemical Reagent	2015100129; CAS: 1310-73-2
N-methyl-2-pyrrolidone	Damao Chemical Reagent	20180424; CAS: 872-50-4
Ester terminated poly(D,L-lactide-co-glycolide) (lactic: glycolic acid = 50:50)	Daigang Biology	DG-50DLGH018
Complete Freund's Adjuvant	MP	0855828
Incomplete Freund's Adjuvant	MP	0855829
Bovine type II collagen	Chondrex	20022
Lipopolysaccharide	Sigma-Aldrich	L2880
Phorbol-12-myristate-13-acetate (PMA) and ionomycin mixture	Multi Sciences	70-CS1001
Critical commercial assays		
TrueSeq RNA library preparation kit	Illumina	RS-122-2001
RNAex Pro Reagent (Total RNA extraction reagent)	AG	21102
Evo M-MLV RT Kit with gDNA Clean	AG	AG11705
SYBR Green Premix Pro Taq HS qPCR Kit	AG	AG11701
Deposited data		
RNA-seq data	This paper	SRA: PRJNA749129
Metadata of Figure 1	This paper	https://doi.org/10.6084/m9.figshare.15087306
Metadata of Figure 2	This paper	https://doi.org/10.6084/m9.figshare.15087642
Metadata of Figure 3	This paper	https://doi.org/10.6084/m9.figshare.15087645

(*Continued on next page*)

Continued

Reagent or RESOURCE	Source	Identifier
Metadata of Figure 4C	This paper	https://doi.org/10.6084/m9.figshare.15087648
Metadata of Figure 4D	This paper	https://doi.org/10.6084/m9.figshare.15087651
Metadata of Figure 5	This paper	https://doi.org/10.6084/m9.figshare.15087702
Metadata of Figure 6	This paper	https://doi.org/10.6084/m9.figshare.15087705
Metadata of Figure S8	This paper	https://doi.org/10.6084/m9.figshare.15087711
Metadata of Figure S9	This paper	https://doi.org/10.6084/m9.figshare.15087714
Experimental models: Cell lines		
RAW 264.7 cells	Laboratory Animal Center of Sun Yat-sen University	NA
Experimental models: Organisms/strains		
Rat: *Sprague Dawley* (SD)	Laboratory Animal Center of Sun Yat-sen University	NA
Oligonucleotides		
Primers for mouse HO1, TCCTTGTACCATATCTACACGG (forward) GAGACGCTTTACATAGTGCTGT (reverse)	Sangon Biotech	N/A
Primers for mouse IL-6, CTCCCAACAGACCTGTCTATAC (forward) CCATTGCACAACTCTTTTCTCA (reverse)	Sangon Biotech	N/A
Primers for mouse IL-1β, TCGCAGCAGCACATCAACAAGAG (forward) TGCTCATGTCCTCATCCTGGAAGG (reverse)	Sangon Biotech	N/A
Primers for mouse TNFα, GCGACGTGGAACTGGCAGAAG (forward) GAATGAGAAGAGGCTGAGACATAGGC (reverse)	Sangon Biotech	N/A
Primers for mouse Hnrnpab, ATCCCAAGTTGAACAAAAGACG (forward) CATACTGCTGTTGCTGATACAC (reverse)	Sangon Biotech	N/A
Primers for rat HO1, TATCGTGCTCGCATGAACACTCTG (forward) GTTGAGCAGGAAGGCGGTCTTAG (reverse)	Sangon Biotech	N/A
Primers for rat IL-6, AGGAGTGGCTAAGGACCAAGACC (forward) TGCCGAGTAGACCTCATAGTGACC (reverse)	Sangon Biotech	N/A
Primers for rat IL-17, CCTGATGCTGTTGCTGCTACTG (forward) TGGAACGGTTGAGGTAGTCTGAG (reverse)	Sangon Biotech	N/A

(*Continued on next page*)

Continued

Reagent or RESOURCE	Source	Identifier
Primers for rat IL-23 CCAGTGTGGTGATGGTTGTGATCC (forward) AGATGTCCGAGTCCAGCAGGTG (reverse)	Sangon Biotech	N/A
Primers for rat Hnrnpab CAGCAACAGCAGTATGGCTCTGG (forward) ACCACGTCGCTGGCTCTTCC (reverse)	Sangon Biotech	N/A
Primers for rat IL-21 AAGGGGCAATGTGAGCACGAAG (forward) CAGGCAGCCTCCTCCTCAGC (reverse)	Sangon Biotech	N/A
Software and algorithms		
Graphpad Prism 8.0	M de Castro Fonseca. et al., 2021	https://www.graphpad.com/scientific-software/prism/

RESOURCE AVAILABILITY

Lead contact

Further information and requests for resources and reagents should be directed to and will be fulfilled by the lead contact, Min Feng (fengmin@mail.sysu.edu.cn).

Materials availability

This study did not generate new unique reagents.

Data and code availability

RNA-seq data have been deposited at SRA (SRA: PRJNA749129) and are publicly available as of the date of publication. Accession numbers are listed in the key resources table. The DOI is listed in the key resources table. Microscopy data reported in this paper will be shared by the lead contact upon request. Accession numbers are listed in the key resources table. All other data have been deposited at Figshare and are publicly available as of the date of publication. DOIs are listed in the key resources table. All data reported in this paper will be shared by the lead contact upon request. This paper does not report original code. Any additional information required to reanalyze the data reported in this paper is available from the lead contact upon request.

EXPERIMENTAL MODELS AND SUBJECT DETAILS

Animal studies

Sprague-Dawley (SD) rats (250-350 g, male, 8-10 weeks old) were used for adjuvant-induced arthritis and collagen-induced arthritis in rats. All animals were maintained under special pathogen free (SPF) conditions and randomly assigned to treatment groups. All *in vivo* studies were carried out in accordance with the Guide for Care and Use of Laboratory Animals which were approved by the Institution Animal Care and Use Committee of Sun Yat-sen University and Guangdong Provincial Hospital of Chinese Medicine.

Cell line

RAW 264.7 cells were obtained from the Laboratory Animal Center of Sun Yat-sen University (LACSYSU) (Guangzhou, China). RAW 264.7 cells were cultured at 37°C with 5% CO2 in complete DMEM supplemented with 10% (v/v) FBS, 100 IU/ml of penicillin and 100 μg/ml of streptomycin. Cells were passaged at ~80% confluence and seeded into 12-well plates at 1×10^5 cells/well.

Primary cells

Single-cell suspensions of rat splenic cells were prepared by filtering the cells with a nylon mesh filter (40 μm) and washing with PBS. After lysis of red blood cells, splenic cells were centrifuged and seeded into a 48-well plate at 1×10^6 cells/well at 37°C with 5% CO2 in RPIM 1640 medium containing 10% (v/v) FBS, 100 IU/ml of penicillin and 100 μg/ml of streptomycin. Cells were incubated with 0.05 μg/ml PMA

and 1 μg/ml ionomycin combining 2 μM monensin overnight, followed by cell counting and adjusting cell density to 1×10^7 cells/ml.

METHOD DETAILS

Evaluation of prophylactic effects of hemin in the AIA model

Sprague-Dawley (SD) rats (250-350 g, male, 8-10 weeks old) were purchased from the LACSYSU. All *in vivo* studies were carried out in accordance with the Guide for Care and Use of Laboratory Animals which were approved by the Institution Animal Care and Use Committee of Sun Yat-sen University. Rats were injected with 0.1 ml CFA in the plantar side of right hind paws at day 0 to establish the AIA model. All animals were maintained under special pathogen free (SPF) conditions and randomly assigned to treatment groups. Rats were then treated with hemin (*i.p.*, twice) at 40mg/kg, 60 mg/kg or 90 mg/kg to determine an optimal dose. To verify the fast-acting prophylactic effects of hemin on acute inflammatory symptoms and arthritis progression, rats were then divided into six groups and treated with hemin at an optimal dose of 40 mg/kg by *i.p.* or *s.c.* injection, or methotrexate at 1 mg/kg by *i.p.* injection, or dexamethasone at 0.225 mg/kg by *i.m.* injection, or celecoxib at 50 mg/kg by *i.g.* administration at 1 h before immunization. All treatments were given twice weekly except that an extra dose of hemin, or celecoxib, or dexamethasone was given at 15 h after immunization. Untreated AIA rats served as the model group. Thickness of right hind paw was measured by a caliper every other day and the clinical scores were graded to evaluate paw swelling, erythema and joint erosions mainly according to the literature (Brand et al., 2007). Photographs of right hind paws were taken at 24 h after immunization to observe the inflammatory symptoms at the peak of swelling. Rats were sacrificed at day 28.

Determination of therapeutic efficacy of hemin in the CIA model

CIA was established following the reported protocol with minor modifications (Liang et al., 2018). Briefly, 2 mg/ml bovine type II collagen was emulsified with IFA at a volume ratio of 1:1 and the final concentration of collagen was 1 mg/ml. At day 0, rats were intradermally injected with 0.1 ml emulsion at the base of the tail and 0.1 ml in the plantar side of the right hind paws. Boost immunization was given at day 7 by injecting with 0.05 ml emulsion at the two sites mentioned above. All animals were maintained under special pathogen free (SPF) conditions and randomly assigned to treatment groups. At day 15, rats were divided into five groups and treated with hemin at 40 mg/kg by *i.p.* injection, or methotrexate at 1 mg/kg by *i.p.* injection, or dexamethasone at 0.45 mg/kg by *i.m.* injection, or celecoxib at 50 mg/kg by *i.g.* administration. All treatments were given twice weekly except that an extra dose of hemin or celecoxib was given at day 16. Untreated CIA rats served as the model group. Paw thickness changes and clinical scores were evaluated every other day as above. Photographs of right hind paws were taken at day 28 after the first immunization and rats were sacrificed for subsequent experiments.

RNA sequencing

Total RNA of liver tissues was extracted with RNAiso Plus and concentrations were measured with NanoDrop Spectrometer (ND-2000; NanoDrop Technologies, USA). Samples were sent to BGI Genomics (Shenzhen, China) for library construction and RNA sequencing (RNA-seq). The library was constructed using Illumina TrueSeq RNA library preparation kit and validated on the Agilent 2000 bioanalyzer (Agilent Technologies, USA). The constructed library was sequenced on the HiSeq 2000 platform (Illumina, USA) and paired-end 100-bp reads per sample were generated. Statistically significant differentially expressed genes (DEGs) with a threshold of FDR;<0.05 and $|Log_2Ratio|>1$ were selected. Venn diagram was generated using the Dr. Tom BGI online supporting system. Heat map showing the expression and hierarchical clustering of overlapped DEGs regulated by hemin was performed by Multi Experiment Viewer (MeV) software (v4.9.0). GO enrichment analysis of DEGs enriched in the immune system process (GO: 0002376) in the hemin-treated group compared with the untreated RA group (RA *vs.* Treated) was performed using Phyper based on the Hypergeometric test. Expression of representative Th1/Th17-related DEGs enriched in the response to stimulus (GO: 0050896) was visualized by the heat map generated by GraphPad Prism 7.0 software, showing the log_{10} (FPKM+1) changes. Data have been uploaded in the National Center for Biotechnology Information SRA database (accession No. PRJNA749129).

In vitro inhibition of proinflammatory cytokines and induction of HO-1

RAW 264.7 cells were cultured at 37°C with 5% CO2 in complete DMEM supplemented with 10% (v/v) FBS, 100 IU/ml of penicillin and 100 μg/ml of streptomycin. Cells were passaged at ~80% confluence and

seeded into 12-well plates at 1×10^5 cells/well. To investigate the anti-inflammatory effects of hemin *in vitro*, cells were stimulated with 500 ng/ml LPS for 6 h and then incubated with 60 μM hemin or 250 nM dexamethasone for 16 h. Total RNA was extracted to evaluate the mRNA expression of IL-6, IL-1β, TNFα, and HO-1 by quantitative real-time PCR (qPCR) as described below.

RNA preparation and qPCR analysis

RAW 264.7 macrophages were collected and total RNA was extracted with RNAiso Plus. Livers, spleens, and inflamed tissues of hind paws of CIA rats were isolated and total RNA was extracted by grinding the tissues in RNAiso Plus at 4°C. After measuring concentration with NanoDrop Spectrometer (ND-2000; NanoDrop Technologies, USA), 1 μg of total RNA was reverse-transcribed into cDNA and qPCR analysis was performed with the high-performance qPCR system (Lightcycler 480; Roche, USA). Relative mRNA expression levels normalized to that of heterogeneous nuclear ribonucleoprotein A/B (Hnrnpab) were calculated by the $2^{-\triangle\triangle CT}$ method. The sequences of primers were listed in the key resources table.

Flow cytometry analysis

Spleens of CIA rats were harvested and grinded under sterile conditions. Single-cell suspensions were prepared by filtering the cells with a nylon mesh filter (40 μm) and washing with PBS. After lysis of red blood cells, splenic cells were centrifuged and seeded into a 48-well plate at 1×10^6 cells/well at 37°C with 5% CO2 in RPIM 1640 medium containing 10% (v/v) FBS, 100 IU/ml of penicillin and 100 μg/ml of streptomycin. Cells were incubated with 0.05 μg/ml PMA and 1 μg/ml ionomycin combining 2 μM monensin overnight, followed by cell counting and adjusting cell density to 1×10^7 cells/ml. Then cells were stained with APC-conjugated anti-CD4 antibody for surface antigen staining. For intracellular staining, cells were incubated with FITC-conjugated anti-IFN-γ antibody after being fixed and permeabilized with Cytofix/Cytoperm Fixation/Permeabilization Solution Kit. The acquisition was performed using the flow cytometer (NovoCyte Quanteon; ACEA Biosciences, USA). Flowjo 7.6 software was used to analyze the data.

Preparation and characterization of the long-acting hemin-ISFI

Hemin-ISFI was prepared by mixing the implant matrix (150 mg PLGA dissolved in 0.3 ml NMP (50% w/v)) and 36 mg hemin powder with two connected syringes. The sufficient mixing of the two parts was achieved by pushing and pulling the syringe piston repeatedly, and the final mixture was injected through one of the syringes. The viscosities and shear stresses of hemin-ISFI and blank implant matrix were measured using the rheometer (Kinexus; Malvern Instruments Ltd., U.K.) with the shear rate ranging from 1 to 100 s^{-1} at 25°C. To confirm the biodegradation of hemin-ISFI, the *in situ* formed implants were isolated at day 10 and day 60 after *s.c.* injection and diameters were measured to observe the changes in dimensions. The scanning electron microscope (SEM) was used to observe the morphology of hemin-ISFI harvested at day 10 after *s.c.* injection. The isolated implants were lyophilized for 24 h (VirTis; SP Scientific, USA), weighted, freeze-fractured, and coated with gold before being imaged using SEM (SUPRA 60; Carl Zeiss, Germany). To evaluate the sustained-release of hemin from the implants, 3 mg of isolated implants was dissolved with 1 M NaOH and the concentration of hemin was measured by UV spectrophotometer (TU-1901; Puxi, China) at 385 nm. Contents of residual hemin in implants were then calculated. Cumulative release proportions were determined by subtracting residual weight from the total mass of hemin in a single formulation.

Investigation of long-acting anti-arthritic effects of hemin-ISFI

To explore whether hemin-ISFI could exert sustained remission of RA, AIA and CIA animal models were established as above. RA rats were injected with hemin-ISFI (*s.c.*) at 120 mg/kg, combining two doses of *i.p.* injections of hemin. Rats treated with methotrexate (*i.p.*) at 1 mg/kg twice weekly served as a positive control. Changes of paw thickness and clinical scores were evaluated every other day as above. Rats were sacrificed at day 28 after adjuvant immunization or day 56 after the first immunization with collagen.

Histological analysis of ankle joints

The ankle joints from healthy rats, untreated CIA rats, and hemin-ISFI-treated CIA rats were collected and fixed in 10% formalin. The joints were decalcified in 15% EDTA for one month, followed by being embedded in paraffin. The sections (4 μm) were cut and stained with hematoxylin-eosin (H&E) and safranin-o. The samples were subjected to immunohistochemistry staining recognizing TNFα, Foxp3, IL-6 and IL-1β. The slides were observed using a digital imaging system (DS-U3; Nikon, Japan) to evaluate

the severity of cartilage erosion, pannus formation, and inflammatory cell infiltration, and expression of TNFα, Foxp3, IL-6 and IL-1β.

QUANTIFICATION AND STATISTICAL ANALYSIS

All statistical analyses were analyzed using unpaired Student's t-test when two groups were being compared or by one-way ANOVA with Tukey post-test for multiple comparisons using Graphpad Prism 8.0 software. All experiments were repeated as indicated in the figure legends. For *in vivo* experiments, *n* represents the number of animals. The error bars in the figures refer to mean ± SD. A *P* value of <0.05 was considered to be statistically significant and significance was displayed as follows: ns, no significance, $*P < 0.05$, $**P < 0.01$, $***P < 0.001$, $****P < 0.0001$.